



NAVAL MEDICAL RESEARCH UNIT SAN ANTONIO

DEVELOPMENT AND VALIDATION OF A PROTOTYPE VACUUM SENSING UNIT FOR THE DD2011 CHAIRSIDE AMALGAM SEPARATORS

JAY SHARTZER, B.S., SOPHIA JOHNSON, PH.D., AND AMBER NAGY, PH.D.

CRANIOFACIAL HEALTH AND RESTORATIVE MEDICINE
BIOMATERIALS AND ENVIRONMENTAL SURVEILLANCE


NAMRU-SA REPORT # 2015-92

Approved for public release; distribution is unlimited.

DECLARATION OF INTEREST

The views expressed in this article are those of the authors and do not necessarily reflect the official policy or position of the Department of the Navy, Department of Defense, nor the U.S. Government. This work was funded by work unit number G1016. Title 17 USC §105 provides that 'Copyright protection under this title is not available for any work of the U.S. Government.' Title 17 USC §101 defines a U.S. Government work as a work prepared by a military service member or employee of the U.S. Government as part of that person's official duties.

REVIEWED AND APPROVED BY:



John Simecek, DDS
Acting Director, Combat Casualty Care & Operational Medicine
Chair, Scientific Review Board
Naval Medical Research Unit San Antonio
3650 Chambers Pass, BLDG 3610
Fort Sam Houston, TX 78234-6315

22 Oct 15

Date



CAPT Elizabeth Montcalm-Smith, MSC, USN
Commanding Officer
Naval Medical Research Unit San Antonio
3650 Chambers Pass, BLDG 3610
Fort Sam Houston, TX 78234-6315

10/26/15

Date

TABLE OF CONTENTS

Abbreviations	4
Executive Summary	5
Introduction	6
Materials and Methods.....	7
Results	21
Military Significance	27
Future Development.....	27
Appendix I: Terminology and Working Definitions	29
Appendix II: Circuit Diagram.....	31
Appendix III: Program Flow Chart.....	32
Appendix IV: Transducer Conversion Compared to RG-1	34
References	35

ABBREVIATIONS

ADC	Analog-to-digital Converter
Ag	Silver
BSPP	British Standard Pipe Parallel
BUMED	Bureau of Medicine and Surgery
CLK	Clock
CS	Chip Select
Cu	Copper
EPA	U.S. Environmental Protection Agency
GB	Gigabyte
GND	Common electrical ground
Hg	Mercury
I ² C	Inter-Integrated Circuit
ISO	International Organization for Standardization
LED	Light Emitting Diode
MISO	Master In Slave Out
MOSI	Master Out Slave In
NPT	National Pipe Thread Taper
POTW	Publically Owned Treatment Works
RG-1	Reference Gauge 1
RG-2	Reference Gauge 2
RTC	Real-time Clock
SCL	Serial Clock Line
SD	Secure Digital
SDA	Serial Data Line
Sn	Tin
SPI	Serial Peripheral Interface
SS	Slave Select
VCC	Voltage Common Connection
VDC	Direct Current Voltage

EXECUTIVE SUMMARY

Background: Dental amalgam is a safe, durable, and effective material frequently used for tooth restorations. Containing up to 50% mercury, amalgam waste created during placement and removal of amalgam restorations can contribute to mercury pollution in waterways. Chairside amalgam separators in dental clinics function as the first line of defense to remove amalgam particulates and debris from dental wastewater through size-exclusion mechanisms. The filtration and retention of particulate over time ultimately affects dental waste evacuation flow rates which can be detrimental to dental procedures. Amalgam separator replacement is performed in timed increments of 2-18 months depending upon manufacturer recommendations. Currently, there are no commercially available amalgam separator units outfitted with an alarming mechanism to alert dental clinicians that their dental waste filtration system no longer operates within manufacturer specification. To address this need, we have developed a vacuum sensing prototype that incorporates an alarm mechanism to denote when the DD2011 chairside amalgam separator does not reach its effective filtering capacity. This research will improve the cost effectiveness of amalgam separators by extending the lifetime of use until its capacity has been reached and will also serve to ensure that dental clinics abide by local, state, and federal mandates for amalgam waste management.

Objective: The goal of this report is to show a proof of concept for an alarm sensor that measures the pressure differential across the amalgam separator. The alarm's audible and visual function will alert the user when replacing the separator is necessary.

Methods: A sensor was built to measure and record differential pressure values within the vacuum lines located on both ports of the amalgam separator. A flow constricting valve was positioned on the outflow port of the DD2011 chairside amalgam separator to induce varying pressure differentials and simulate vacuum line blockage due to amalgam waste and dental debris. Data generated from the transducers during simulated blockages were transformed into pressure values using linear regression equations from the calibration data.

Results: The greatest divergence in differential pressure was observed when the flow constricting valve was rotated from a fully open position (0°) to a position between 30° - 60° . Obstructions beyond the 30° position induced a differential pressure that exceeded predetermined differential pressure limit triggering the visible and audible alerts within the sensor.

Conclusions: The simulated obstruction separator experiments validated the sensor's ability to detect differential pressure changes and alert the user of flow impediment through visual and audible cues.

INTRODUCTION

Although the proportion of amalgams placed has decreased from approximately 50% in 2003 [1], to between 37-42% in the past decade [2], [3], amalgam waste is still an environmental concern. Amalgam is composed of liquid mercury (Hg) and an alloy powder consisting silver (Ag), tin (Sn), and copper (Cu) [4]. Dental clinics can produce up to 4.5 g of Hg per day, which approximates to 1 kg per year [5]. Although releases of Hg from individual clinics are not considered to be the major contributors to the overall Hg burden in wastewater, the cumulative effect of Hg release from all dental clinics is known to be significant [6].

In 2003, 50% of all Hg contamination entering publically owned treatment works (POTW) was attributed to dental amalgam [7], [8]. An estimated 122,000 dental offices have discharged amalgam into POTW for a total discharge approximation of 3.7 tons of Hg per year [9].

Amalgam separators offer a cost-effective and efficient means of controlling Hg discharge into POTW. This amalgam waste management practice removes up to 99% of Hg from waste streams [10]. Separators function by using sedimentation, filtration, centrifugation, chemical, or a combination of these removal mechanisms to eliminate amalgam particulates from dental wastewater. A benefit of filtration amalgam separators is that they function without the use of moving parts, which reduces the cost and the probability of mechanical difficulties [11]. Chairside amalgam separators, such as the DD2011, remove amalgam waste particulates by filtration and are attached to the vacuum system of dental chairs for easy removal and replacement. Amalgam particulates captured by manufacturer-installed, chairside amalgam traps prevent vacuum line blockage by removing large dental waste deposits and tooth debris [12]. This makes chairside amalgam separators a preferable option as a first line of defense for the removal of dental amalgam waste. In addition, separators aid in preserving the wastewater plumbing of dental clinics by preventing sludge build up over time.

Chairside amalgam separator replacement schedules are currently independent of the volume of amalgam waste entering the filtration device and solely dependent upon a set service schedule. Time-based determination of the amalgam separator lifespan does not address variability between individual amalgam separators as well as outlying events that may critically disrupt the separator's efficiency. Unforeseen challenges, such as damage to the filtration medium or debris buildup within the inflow and outflow ports, could disrupt the fluid flow and prematurely reduce the suction force necessary to collect amalgam and biomaterial from a patient's oral cavity.

To ensure a properly functioning amalgam separator that performs within current and proposed government mandates, a user-friendly sensor is necessary to monitor the differential pressure across the separator that immediately reports adverse conditions. The objective of this research was to design, build, and validate a vacuum sensing prototype that records changes in pressure differentials and provides an audible and visible cue when vacuum pressure drops below predesignated levels necessary for proper dental suction. These data will allow dental clinics to achieve full utilization of amalgam separators in addition to remaining in compliance with amalgam waste management regulation.

MATERIALS AND METHODS

Materials

Included below are the manufacturer and procurement information for the materials used to develop the vacuum sensor. The power supply for Samsung SyncMaster LCD/TFT 770 was manufactured by SIB-CORP (Clifton, NJ). The Adafruit data logging shield was manufactured by Adafruit (New York City, NY). The Arduino Uno Rev3 microcontroller was manufactured by Arduino LLC (Turin, Italy). The Secure Digital (SD) card was a Kingston 4 GB microSDHC Class 4 SDC4/4GBET Flash SD card (Fountain Valley, CA). Carbon resistors with a 1% tolerance were acquired from a 1/4W 86 Value 860 piece resistor kit set manufactured by Joe Knows Electronics, LLC (Taylors, SC). The heat-shrink tubing was manufactured by Vktech (Stockholm, Sweden). Gardner Bender manufactured (Menomonee Falls, WI) the LTB-400

black liquid electrical tape used. Jumper wires were either used from the Elenco JW-350 jumper wire kit (Wheeling, IL) or from Dupont's 3 x 40 piece jumper wire set, model number RR40DUP. Non-lead solder was supplied by Rosewill (City of Industry, CA) in their RTK-090 tool kit, which is sold by Amamax (Houston, TX). All of the previously mentioned materials were purchased through amazon.com. Swagelok PTI-S-JS0-31BJ-BX transducers, along with connecting cables, were purchased from Swagelok Austin (Austin, TX). Ashcroft KXF01100-1/0BAR=M04FM1 transducers along with connecting cables were purchased from BriceBarclay (Stafford, TX). Type 316 stainless steel female National Pipe Thread (NPT) solid tees and Female British Standard Pipe Parallel (BSPP) solid tee consisting of carbon steel with anti-corrosive plating were purchased from Discount Hydraulics (Philadelphia, PA). NW/KF 25 flange to male 1/2 inch NPT thread adapters and NW/KF 25 to 1 inch hose adapters were comprised of 304 stainless steel and purchased from Ted Pella (Redding, CA) along with an aluminum NW/KF 25 flange to 1/2 inch or 5/8 inch hose adapters. Stainless steel worm gear clamps (9/16 to 1-1/16 inch) and 1/2 inch Freeman Teflon tape were purchased through Global Industrial (Buford, GA). KF 25 flange adapter to 1 inch male BSPP, aluminum toggle clamp with cotter pin for flange size KF 25, and KF 25 stainless steel centering ring vacuum with Viton[®] O-rings were purchased from Ideal Vacuum Products (Albuquerque, NM). Plastic housing for the sensor case, light emitting diode (LEDs), USB A to B connector, button switch, electronic spacers, protoboard, screw terminals, piezoelectric buzzer, and banana plug screw connectors were available as stock materials during development.

Methods

All measurement units of pressure were converted to inches of Hg using published conversion factors [13].

The sensor can be subcategorized into three major units: sensing, datalogging, and alarm. These components are illustrated conceptually in Figure 1.

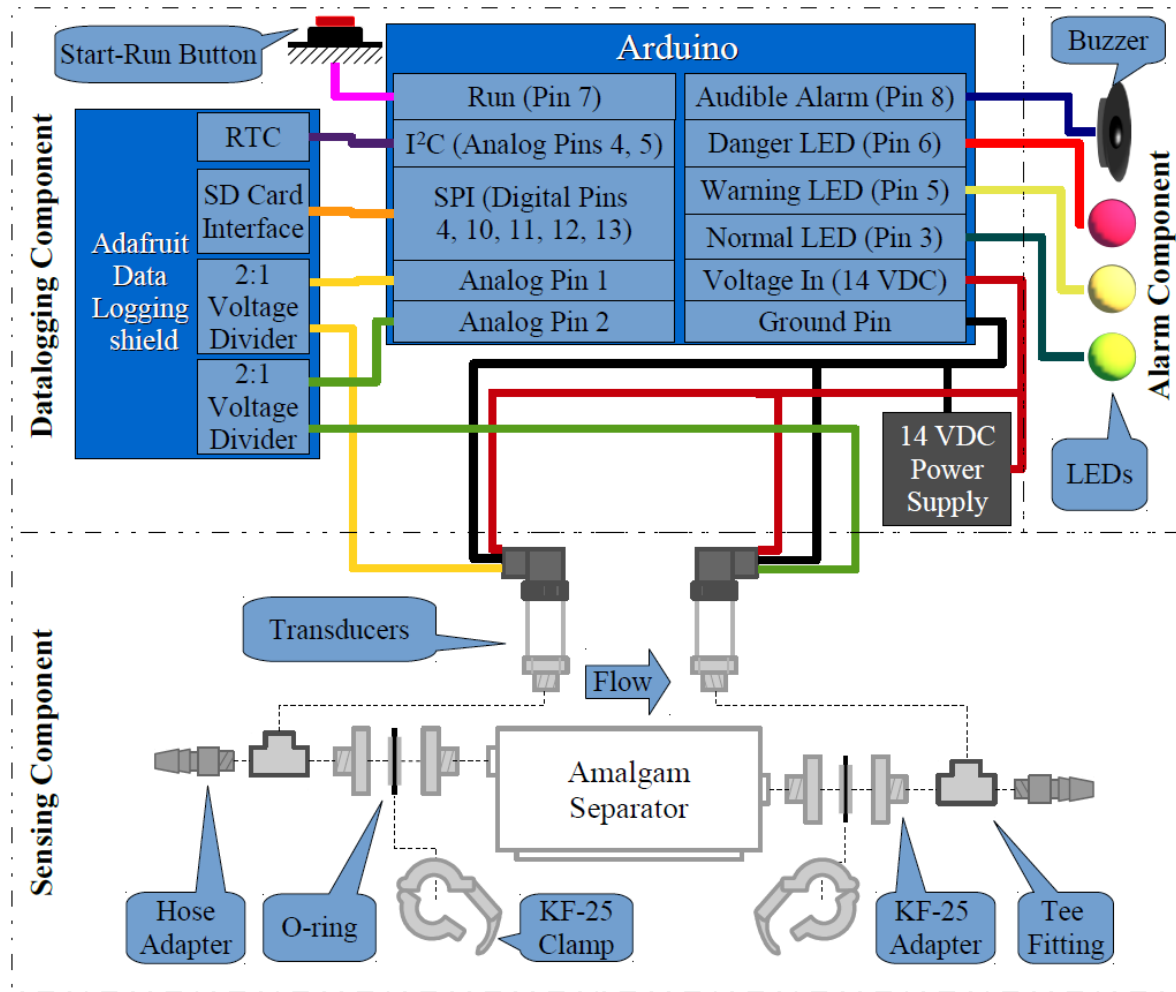


Figure 1. Graphical diagram of the sensing, datalogging, and alarming components of the sensor. Figure is not to scale.

A. Sensing Component

1) **The Ashcroft KXF01100-1/0BAR=M04FM1 transducer**, identified by an oval in Figure 2, converts an applied pressure on its diaphragm ranging between -7.36 inches of Hg (-100 kPa) of vacuum and atmosphere to a voltage between 0 and 10 direct current voltage (VDC) [14]. The transducer installed on the dental cart in Figure 2B was used during the simulated blocking experimental setup. The Ashcroft transducers are threaded with 1/2 inch National Pipe Thread Taper (NPT).

2) ***The Swagelok PTI-S-JS0-31BJ-BX transducer***, identified by a square in Figure 2, was constructed to use a voltage source of 14 to 30 VDC [15]. The Swagelok pressure transducer measured -7.36 inches of Hg (-100 kPa) of vacuum to atmosphere and translated that pressure to a range of 0 to 10 VDC as a signal output. The Swagelok used a male fitting of 1 inch BSPP thread and attached to a pipe fitting of comparable female thread. While equal in performance, the Ashcroft transducer was selected over for the Swagelok transducer in further validation of the sensor as the former has a smaller footprint. Figure 2C illustrates the installation of the Swagelok transducers on a dental chair.

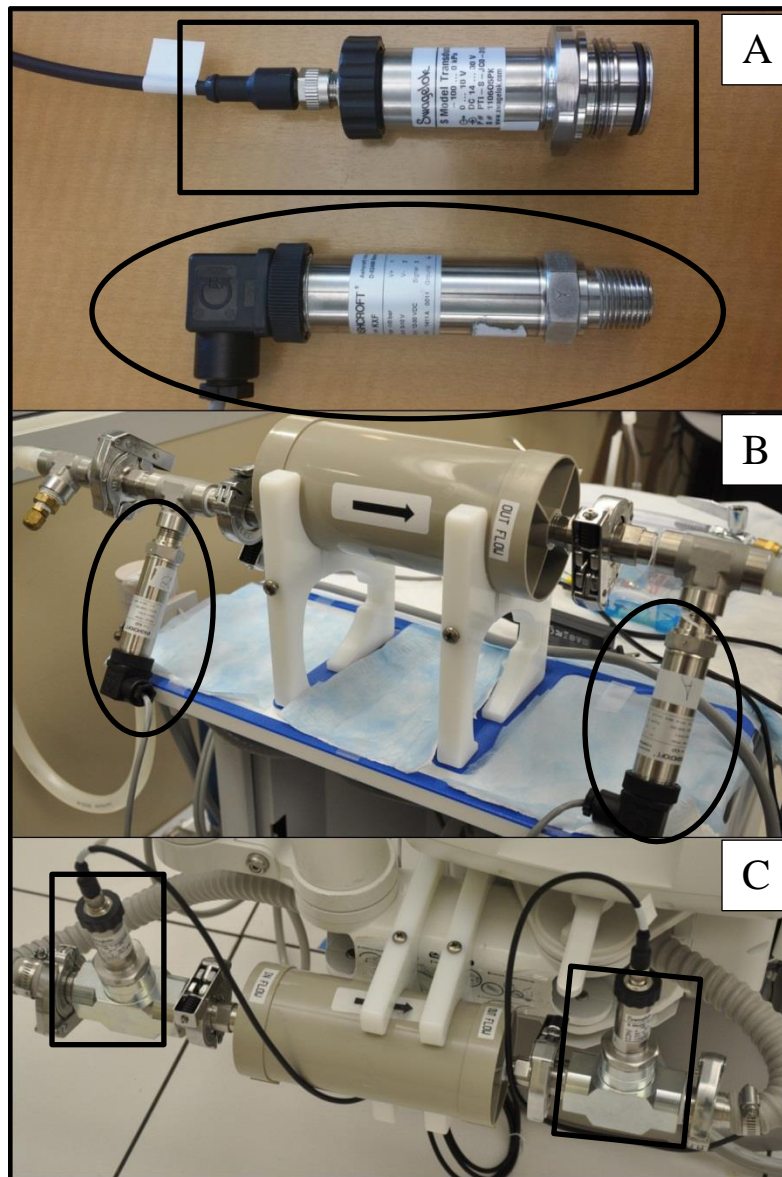


Figure 2. A) Swagelok (square) and Ashcroft (oval) transducers. B) Installed Ashcroft pressure transducers on the mobile dental cart for prototype sensor validation experiments. C) End-use scenario installation of Swagelok pressure transducers on a dental chair.

3) *A variety of fitting types* were used to connect two transducers to the amalgam separator and subsequently the inflow and outflow dental vacuum tubing. The fittings aligned each

transducer perpendicular using female-ended tees. Then each tee was connected in line with the amalgam separator as well as the dental vacuum tubing using quick release K-F flange vacuum adapters that were secured with Viton[®] O-rings and flange clamps. The fitting's assembly is graphically represented in the sensing component of Figure 1 and the configuration of each transducer is illustrated in Figure 2.

B. Data logging component

The datalogging component converts the pressure transducer output to digital data which is then stored on the SD card. Figure 3 presents the complete datalogging component during various stages of assembly. This component consists of an Arduino Uno Rev3 microcontroller, an Adafruit data logging shield, a 4 GB SD card, a data collection start button, a power source, and a voltage divider.

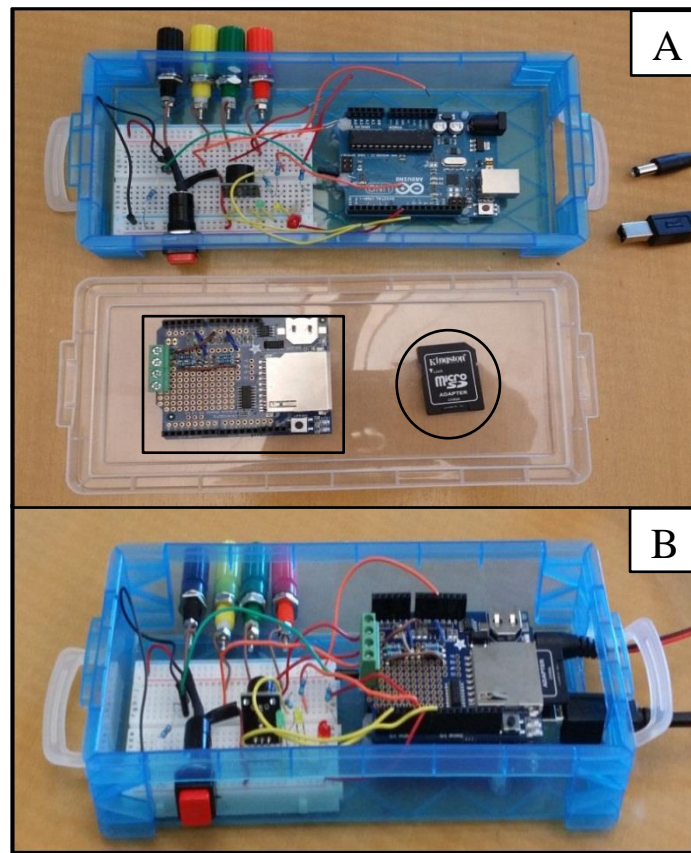


Figure 3. The datalogging component of the sensor A) with the Adafruit Data Logging Shield (square) and SD card (circle) disassembled, and B) fully assembled without the cover.

4) *The Arduino Uno Rev3 microcontroller* shown in Figure 4 is a multi-use programmable microcontroller with digital input/output pins, analog inputs, onboard clock, and reset button. A detailed diagram of the analog inputs and digital input/output pins are in Figure 14 located in Appendix II: Circuit Diagram.

The Arduino microcontroller is programmed using a subset of the programming language C++ and interfaces with the Arduino IDE software [16]. Within Appendix III: Program Flow Chart, Figures 15 and 16 represents the flow of data collection from the program initialization until all data is written onto the SD card. The figures show the program running the Arduino conceptually and without the syntax of C++. The program begins with checking the SD card for errors and waiting for an indication from the user to begin data collection. Once such indication is made, the program instructs the Arduino to create a text file on the SD card and begin data collection. Communication with the SD card is performed using the serial peripheral interface

(SPI) communication protocol. Another communication protocol standard employed is Inter-Integrated Circuit (I²C) [17]. The I²C communication protocol uses the analog input pins on the Arduino board to read time values from the real-time clock (RTC) and link the digitally-converted transducer readings to the exact time they were collected. The Analog-to-digital Converter (ADC) modified transducer data is continuously paired with the time of data collection and written to the newly created text file until the power is lost or the user resets the Arduino.

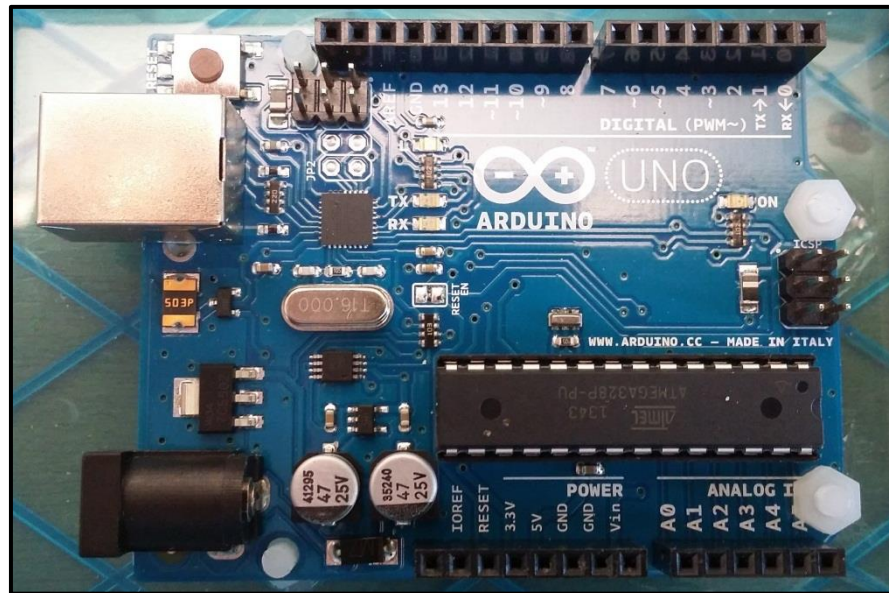


Figure 4. The Arduino Uno microcontroller functions as central component of the datalogger. This device controls the flow of information received from the pressure transducers and RTC, activates the alarming components, and formats the output data to the SD card.

5) *The Adafruit data logging shield*, seen in Figure 5, provides an interface for the onboard RTC and SD card slot on top of the Arduino microcontroller. In general, Adafruit shields are expansions to the Arduino microcontroller that interface directly with the input/output and analog pins. The direct link between the Adafruit shield and microcontroller allows the transcription of time-stamped, raw pressure values onto the SD card. The addition of free and open-source Arduino libraries allowed for the seamless integration of the shield into the sensor source code.

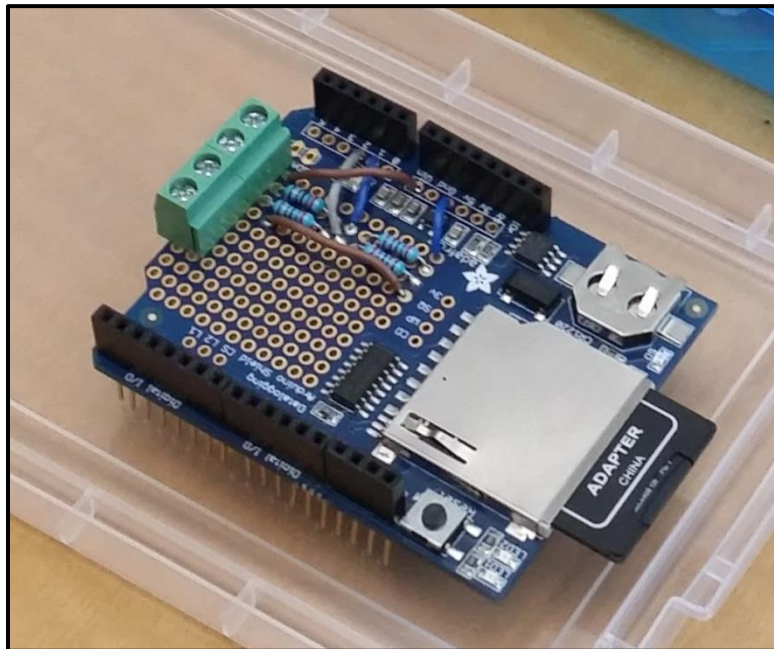


Figure 5. Adafruit data logging shield with inserted SD card. The SD card saves data and time values concatenated on a delimited string of data. The data logging shield also contains the RTC which provides the Arduino with real-time values.

6) *AC Adapter/Charger Power Supply for a Samsung PSCV420102A SyncMaster LCD/TFT monitor* was repurposed to supply power to the vacuum sensor. The maximum input voltage for the power supply is 240 volts, which was converted into 14 VDC up to 3 amps. The electrical conductivity of 14 voltage output was confirmed with a multi-meter after modifying the plug connection to the Arduino.

7) *The voltage divider* splits the input voltage into two output voltages of a desired ratio [18, p. 61]. The addition of a voltage divider reduces the expected 0 to 10 input voltage signal produced by the transducer to an Arduino compatible 0 to 5 voltage signal, Figure 6. For the construction of this prototypic vacuum sensor, the desired ratio of input : output voltage was 2:1.

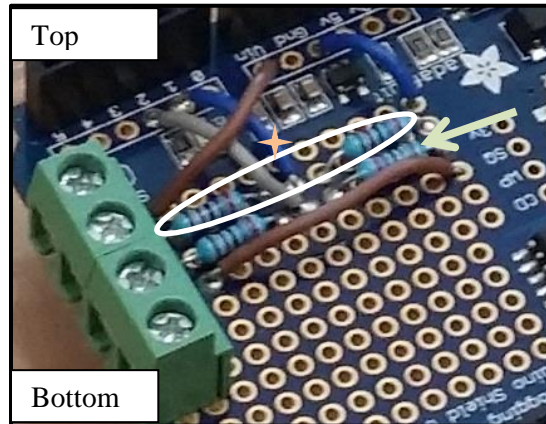


Figure 6. Voltage divider location on the Adafruit data logging shield. All references are made from top to bottom. The top brown wire and screw terminal connects the pressure transducers with the 14 volts in direct current power supply. The pair of resistors (oval), and blue wire (orange star) provides the 2:1 voltage division for the inflow transducer to the Arduino's Analog Pin 1. The bottom pair of transducers (arrow), the third screw terminal, and grey wire provides the 2:1 voltage division for the outflow transducer to the Arduino's Analog Pin 2. The brown wire at the bottom of the picture and the last screw terminal provides the electrical common ground for the transducer.

C. Alarm Component

Audible differential pressure set points were determined with reference to the International Organization of Standardization compliance flow rate requirement of 1L/min. A liter of water evacuated within 1 min, 1.5 min, and greater than 2 min were categorized as normal, warning, and critical states respectively. The recorded pressure differentials for each alarm state were greater than -4.0 (normal), between -4.0 and -8.5 (warning), and less than -8.5 (critical) inches of Hg. The flow rate was constricted using a regulator valve at the outflow port on the amalgam separator. Normal, warning, and

critical audible alarm differential pressure states correspond to green, yellow, and red visual LEDs of the alarm component.

The audible aspect of the alarm was achieved by attaching a piezo buzzer to the Arduino. Both the LEDs and the buzzer can be seen left of the start run button in Figure 7. The buzzer was programmed to sound when the critical LED illuminates. In addition, a function was added to turn the alarm audible on and off by holding the start-run button for more than a second during operation.

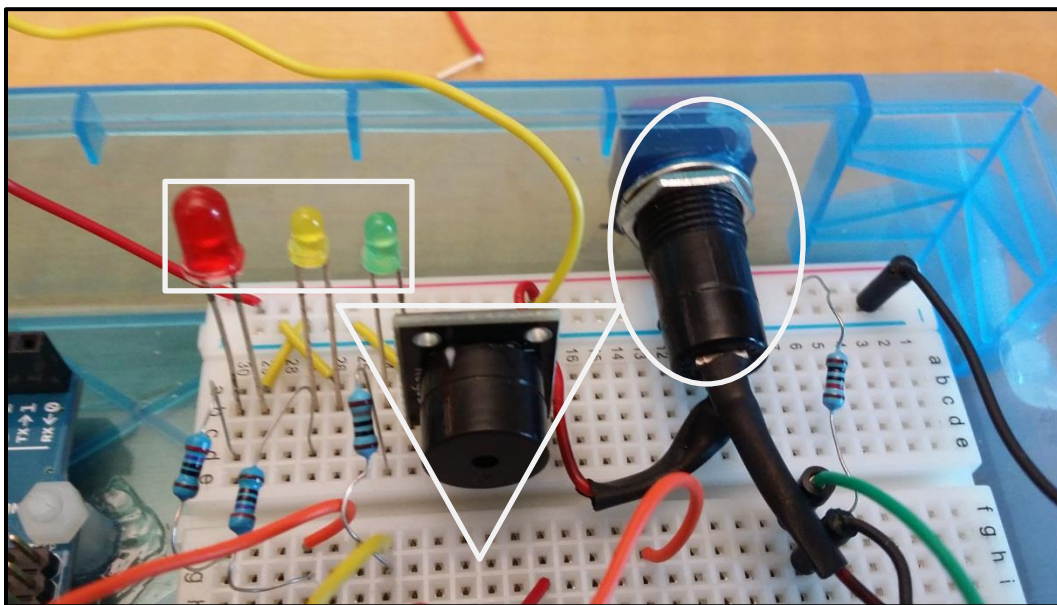


Figure 7. The buzzer (triangle), LEDs (rectangle) and start-run button (oval) elements of the alarm component.

Transducer Calibration

Transducers were calibrated using a reference gauge over a range of pressure values at a consistent vacuum flow. This was accomplished by creating the same set-up as seen in Figure 8, which allowed for nearly the same pressure induced simultaneously on both the transducers and reference gauge diaphragms. An Ashcroft gauge with a pressure range from 0 to -7.36 inches of

Hg (0 to -100 inches of H₂O), henceforth referred to as Reference Gauge 1 (RG-1), was used to infer the linear relationship between the transducer output and the vacuum pressure. A 0 to -14.71 inches of Hg (0 to -200 inches of H₂O) Ashcroft gauge, henceforth referred to as Reference Gauge 2 (RG-2), served to validate RG-1. RG-2 ensured that RG-1 functioned adequately given that unusually high differences between the two gauges would signify that one of the gauges was malfunctioning.

Once the calibration rig was operational, a flow constricting valve was manipulated to allow for unobstructed flow and the vacuum pressure was increased to a point just below -0.74 inches of Hg (-10 inches of H₂O). The calibration setup is presented in Figure 8. The vacuum pressure changed according to the adjustment of the flow constricting valve. The recorded pressure ranges for RG-1 were -1.103 to -6.988 inches of Hg (-10 to -90 inches of H₂O) and are recorded in Table 1 in Appendix IV: Transducer Conversion Compared to RG-1. A linear regression analysis was conducted to establish a relationship between the gauge pressure and the ADC conversion of the transducer output. Specifically, the trendline information (slope and y intersect) of the averaged values from three independent calibration curves generated with the reference gauges were used to convert the ADC output to equivalent pressure values in inches of Hg. For example, the inflow calibration curve (Figure 9) linear equation was calculated as $Y = 34.67 \times X + 1059$; therefore, the inches of Hg for the inflow ADC output equaled $(\text{inflow} - 1059) / 34.67$.

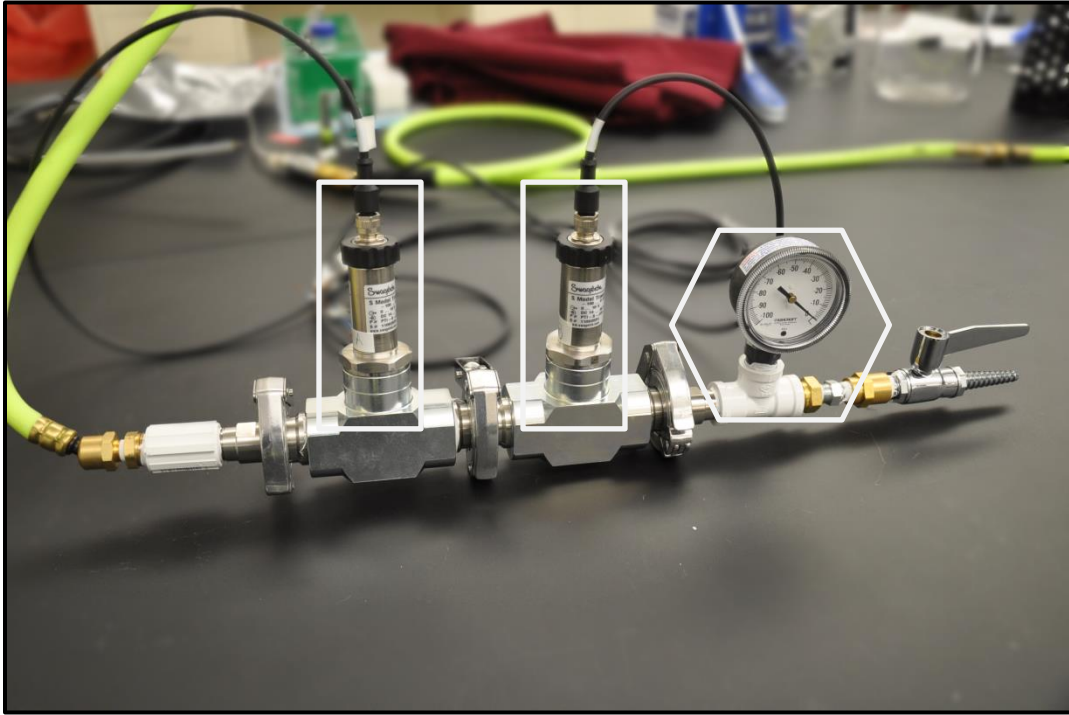


Figure 8. Calibration rig setup of the Swagelok pressure transducers (rectangle) with RG-1 (hexagon). The Ashcroft and Swagelok transducer calibrations were completed in an equivalent manner.

Data Resolution

The ADC of the Arduino has a 10-bit ADC which equates to 1024 states that can be used to digitally approximate an analog signal. For example, an ADC output of 0, 550, or 1023 is equivalent 0, 2.68, or 5 VDC, respectively. Given that the pressure ranges for both transducers are atmosphere to -7.36 inches of Hg, the resolution of the ADC can be calculated to be 4.88 (millivolt / state) \times 7.36 (inches of Hg) / 5 volts = 0.00718 inches of Hg per state. The previously mentioned equation does not factor in noise from electrical or fluidic sources; thus, a calibration file was required to create a reliable relationship between the transducer output and pressure values.

Data Code and Collection

The Arduino collects date information from the RTC and creates text files on the SD card titled with the date and time that the experiment began. Inside this text file, the Arduino assigns the date and time on the first line in ISO 8601 format [19]. The pressure signals from the inflow and outflow transducers are converted into a digital step range from 0 to 1023 by the microcontroller, and paired with the time point registered by the RTC presented on the Adafruit data logger. The inflow and outflow signal ranges along with the corresponding time points are appended to a delimited table in a text file located on the SD card. Data collection continues until the user unplugs the power supply to the Arduino or the Arduino's reset button is pressed.

Amalgam Separator Obstruction Simulation

A DD2011 chairside amalgam separator obtained from Dennis J. Duel Associates, Incorporated (Chicago, IL) was installed on the mobile dental cart (AMC-20CE, Aseptico Inc., Woodinville, WA, USA) as shown in Figure 2B. To test the prototypic vacuum sensor, an obstruction was simulated by installing a flow constricting valve to the outflow port on the amalgam separator. Narrowing the outflow port cross-sectional area on the DD2011 chairside amalgam separator allowed for the controlled resistance to be applied across the transducer diaphragm over preset angles. These angles were determined using a protractor for the following restriction positions: 0°, 15°, 30°, 45°, 55°, and 60°. The 90° position was not tested because it completely constricted fluid flow. Differential pressure values were obtained for the aforementioned restriction angles. The experimental procedure outlined below served to mimic a natural obstruction in a controlled manner.

A high vacuum evacuation device was used to flush a liter of tap water through the system. The time that flushing began and ended was recorded. The high vacuum evacuation device valve remained open until all water was collected in a vessel before

placing it in its holder. The ADC output from four independent trials for each obstruction position were converted into pressure readings using the linear regression equation generated from the data presented in Figure 9.

RESULTS

Calibration

The relationship between the pressure induced on each of the transducers and values read by the ADC on the Arduino was delineated during the calibration of the sensor. The data for the calibrations between the Ashcroft and Swagelok pressure transducer with RG-1 are presented in Figure 9. From this data, the transducers are assumed to have equivalent performance based upon similar pressure output values and a $p > 0.05$. The more manageable Ashcroft transducers were chosen for the remaining experimental studies that validated the performance of the vacuum sensor in a practical and relevant scenario.

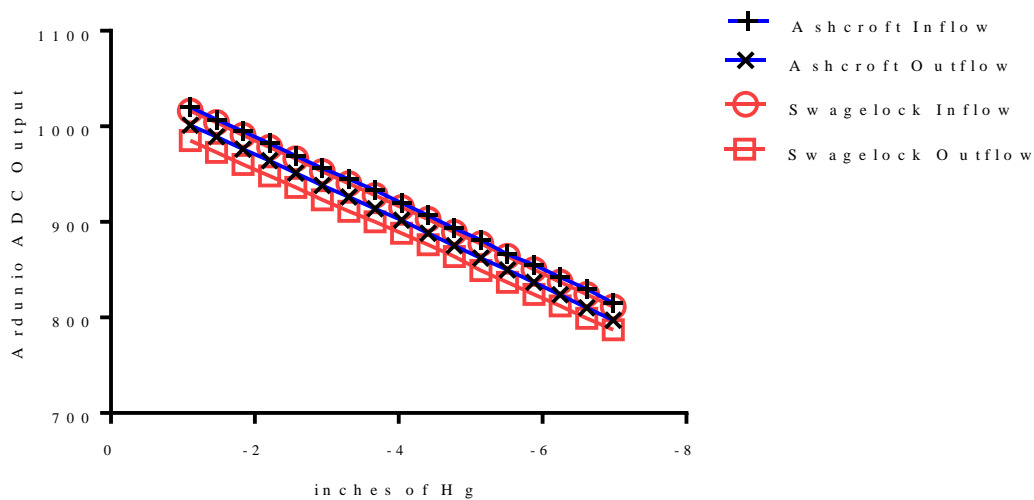


Figure 9. Linear regression analysis of Ashcroft (filled shapes) and Swagelok transducers (unfilled shapes) calibration using RG-1. The R^2 value for each curve was greater than 0.9997.

Within an isolated system, the ADC conversion of the Ashcroft transducer output was compared with the pressure readings for each reference gauge as seen in Figure 10. Since both reference gauges outputted similar values, it was confirmed that the reference gauges' calibration were still valid, $p > 0.05$.

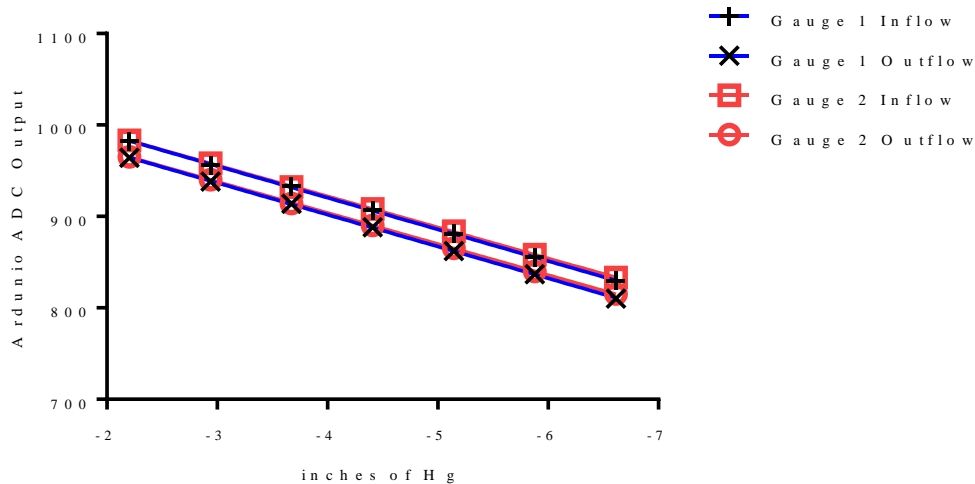


Figure 10. Comparison of RG-1 and RG-2 versus Ashcroft transducer to illustrate a negligible difference in the output values for both reference gauges.

Sensor Detection of Simulated Obstructions

To test the function of the vacuum sensor setup, hardware, and software, a flow constricting valve was attached to the outflow port of the DD2011 chairside amalgam separator located on a mobile dental cart. Changes in differential pressure, the difference between the outflow and inflow pressure values, were first tested by introducing one liter of water into the system with a completely open constricting valve.

An illustration in differential pressure for an unobstructed separator is shown in Figure 11. The introduction of water into the vacuum sensing system can be divided into four discreet stages. Stage one represents the initial pressure drop when water was introduced to the system. In stage two, the pressure drop had a characteristic inflection

point, which was usually approximately -4.0 inches of Hg. Stage three was denoted by a rise in pressure drop from -4.0 to 0 inches of Hg. Lastly, stage four corresponded to a stationary state where the inflow and outflow pressure readings stabilized and returned to baseline levels.

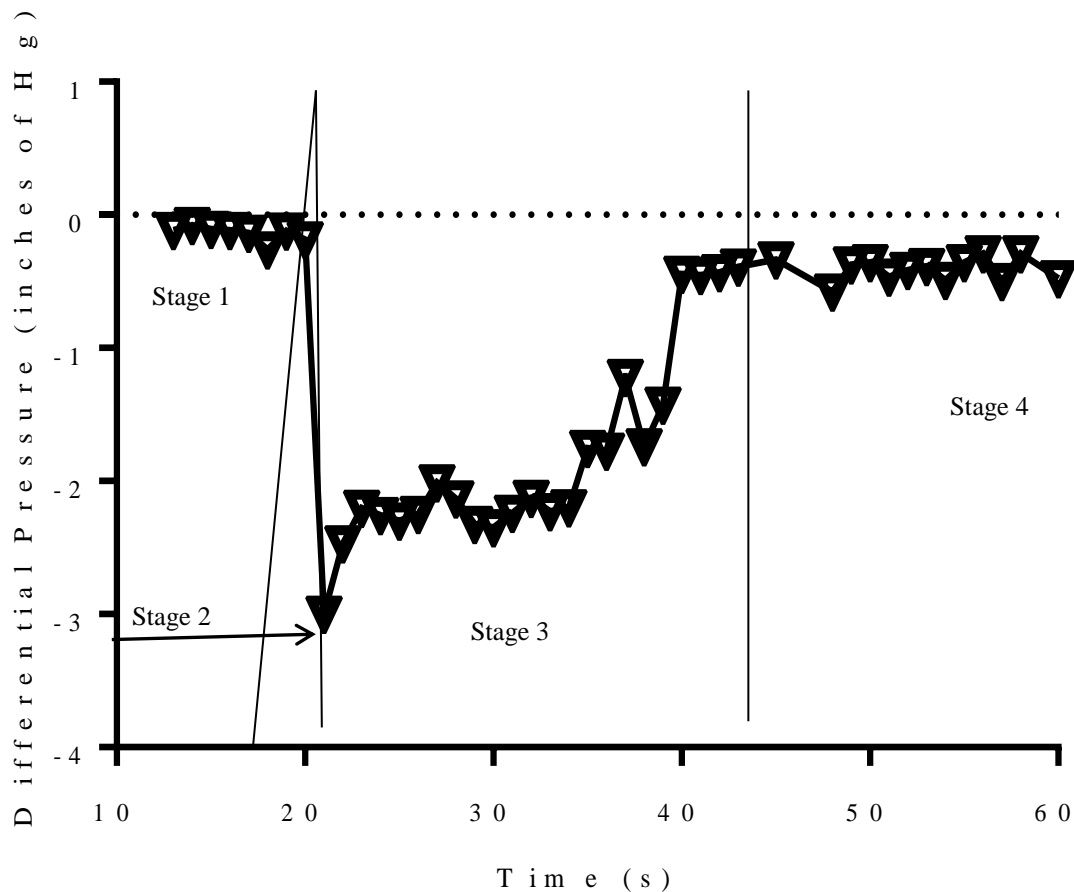


Figure 11. Stages of differential pressure after introducing water into an unobstructed DD2011 chairside amalgam separator using Ashcroft transducers.

To simulate DD2011 chairside separator blockage, a constricting valve was positioned between 0° and 90° where 0° corresponded to a fully open valve and 90° corresponded to a closed valve. When water was first introduced into the vacuum lines, the maximum resistance for flow across the filter was reached. Reduction in the differential pressure as a function of flow restriction was not initially apparent until the separator's cross-sectional area was restricted to

the 45° position. The magnitude and consistent decline in the differential pressure throughout the data collection timeframe for measured obstruction positions resulted in a distinct output trend identifying a partial (45°) and total flow restriction angle (60°), Figure 12. As water exits the separator, the water flow resistance decreased as the pressure on the transducers' membrane was reduced. This observation was apparent in all valve closure positions excluding 60°. The obstruction at 60° maintained a high membrane resistance, which prevented the inflow and outflow pressure readings from equalizing. For all flow restriction conditions, stage four baseline levels were reached earlier in unobstructed rather than obstructed amalgam separator.

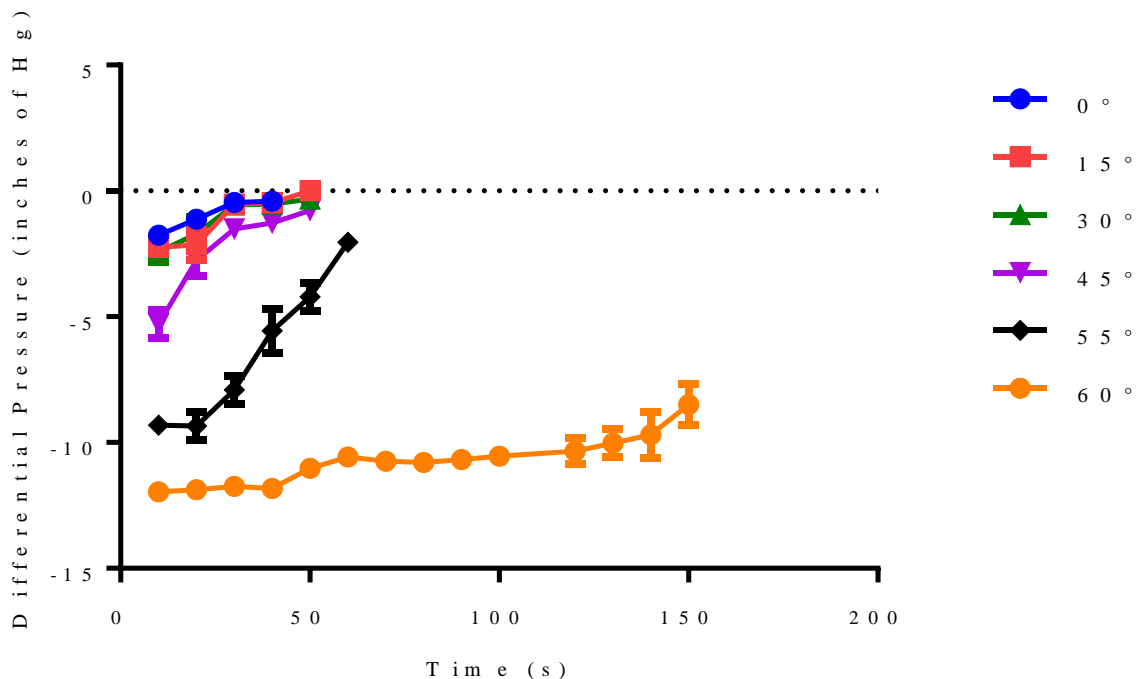


Figure 12. Ashcroft differential pressure comparison of 0° (blue), 15° (red), 30° (green), 45° (purple), 55° (black), and 60° (orange) positions during stage 3 and 4 of the pressure drop. The values given represent the mean \pm 0.6 inches of Hg of four independent replicates.

The increased resistance across the amalgam separator was proportional to the forced reduction in flow rate. At or before the 30° valve position, the differential

pressure change was negligible but the flow rate gradually declined to 20% of an unobstructed flow rate, Figure 13. The differential pressure doubled when water flow was restricted by closing the valve between positions 45° and 60°, reducing the flow rate by 80% compared to unobstructed flow (Figure 13). These trends infer an inverse relationship between the differential pressure and flow rate.

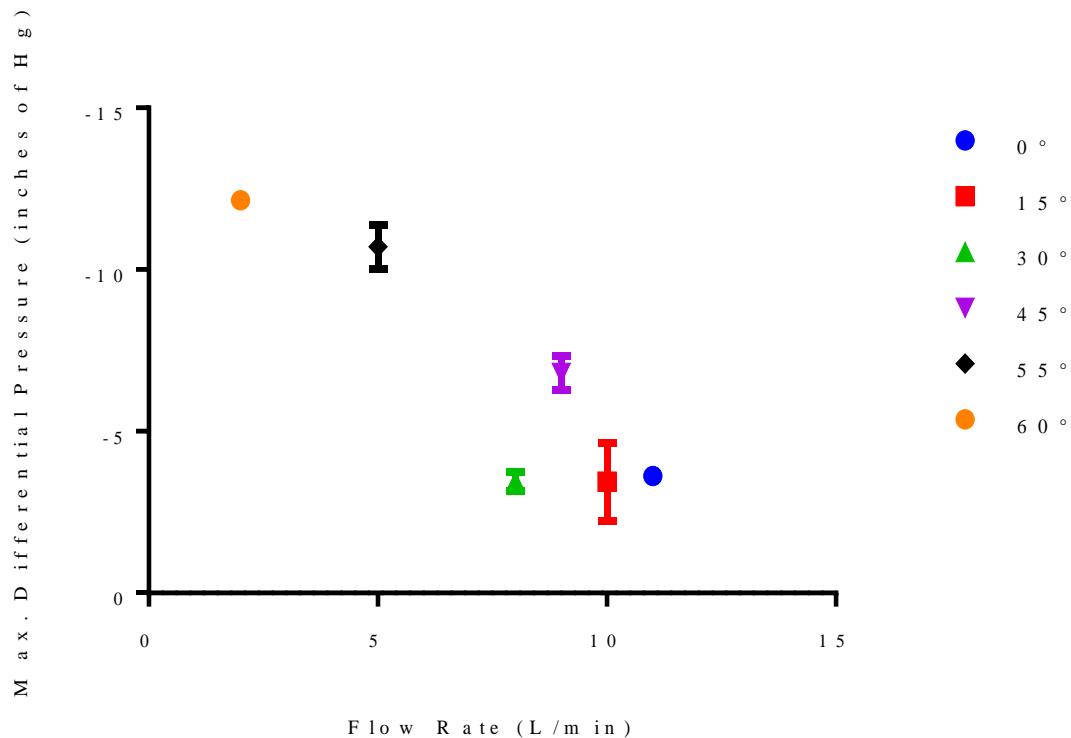


Figure 13. Obstructed flow rate at 0° (blue), 15° (red), 30° (green), 45° (purple), 55° (black), and 60° (orange) positions as a function of differential pressure ± 1.0 inches of Hg.

Varying flow rates for a liter of water to pass through the amalgam separator corresponded to the built-in audible and visual differential pressure set points. The LED visual alarm switched from normal to warning mode as the differential pressure decreased beyond -4.0 inches of Hg during and immediately after flushing one liter of water through the system at a

restriction angle of 45°. After activating the high evacuation device, the warning LED was succeeded by the critical (differential pressure less than -8.5 inches of Hg) LED upon suctioning water through the system at an impediment angle position of 55°. The critical LED remained illuminated and a continuous audible alarm sounded since the differential pressure remained outside the preset pressure limit when the water flow was restricted to a 60° position. Together, these data demonstrate proof-of-principle that an effective, sensitive vacuum sensor can be constructed to monitor flow rates and differential pressure of the DD2011 chairside amalgam separator.

Conclusion

Commercially available amalgam separator units lack in-situ performance monitoring and suitable replacement notification mechanisms. The purpose of this research was to construct a prototypic vacuum sensor that continuously monitored pressure differentials and triggered audible and visual alarms when a large differential indicated excessive amalgam separator obstruction. This approach is based upon the principle that solid particulate amalgam waste and dental debris accumulate and block the movement of water through the filtration medium thereby reducing the flow rate. By monitoring and recording flow rate data, chairside amalgam separators will be used to its effective lifespan, which is predicted to save time and be more cost effective. In this report the design, calibration, and validation of a prototypic vacuum sensor is described. Two pressure transducers, Ashcroft and Swagelok, were shown to measure pressure across the amalgam separator and provided adequate sensitivity during calibration testing. However, the Ashcroft transducers were chosen for subsequent vacuum sensor validation tests due to their smaller footprint. To simulate particulate and dental debris obstruction in vacuum lines, a flow constricting valve was situated at the outflow port of a DD2011 chairside amalgam separator installed on a mobile dental cart. The vacuum sensor successfully detected and recorded simulated obstruction, which was demonstrated by the inverse relationship between flow rate and pressure differential as the flow

constricting valve closed. In addition, the datalogging and alarm sensing components were found to function as programmed with both an audible and visual alarm when the flow obstruction exceeded designated warning and critical levels.

Together, these data provided evidence for the successful design and execution of a vacuum sensing unit that has applications like dental wastewater effluent monitoring. It is anticipated that this research will lead to the development of more efficient and effective dental amalgam separator systems that include monitoring and alarm features. The availability and deployment of second generation dental amalgam separators that have self-contained monitoring and alert systems will improve environmental compliance efforts ahead of the EPA proposed ruling on management of dental amalgam waste.

MILITARY SIGNIFICANCE

To further support nationwide Hg abatement efforts, the Navy issued Bureau of Medicine and Surgery (BUMED) instruction 6260.30 mandates the use of amalgam separator systems in dental treatment facilities. However, with more stringent dental amalgam waste regulation on the horizon, it has become necessary to maximize the full potential of amalgam separator systems. This includes improving filtration efficiency and utilizing separators to their maximum effective lifespan. Therefore, the Navy has addressed the latter of these issues through development of a prototypic vacuum sensor that can monitor and detect differential pressure across chairside amalgam separators. The sensor alerts personnel if the suction force becomes substandard. This technology is expected to help all military branches by reducing the financial burden associated with replacing amalgam separators according to manufacturer's assumed versus observed unit lifespan. The sensor also has potential use in other applications that require vacuum line monitoring.

FUTURE DEVELOPMENT

The development of a vacuum sensor outfitted with a datalogging unit and alarm feature is an excellent initial effort to improve management of dental amalgam separator systems. While

the sensor described in this study has certainly demonstrated its functionality under ideal test conditions, additional experiments are necessary to determine if it can perform under more strenuous laboratory conditions as well as in the clinic. In upcoming studies, this prototype will be subjected to dental wastewater that contains an appreciable amount of dental amalgam waste and dental debris. It is expected that the effective lifetime of DD2011 chairside amalgam separators will be better delineated by introducing the sensor into a more complex test environment. Deployment of this sensor prototype in the clinic will undoubtedly bring to light important functional and executional issues that cannot be identified by laboratory experimentation. Additional research will be performed to lower costs associated with sensor construction, including testing flow switches as an alternative to pressure transducers. Further, an ADC with substantially greater accuracy and a more user-friendly interface could be introduced into the datalogging component. The use of a more precise ADC, which would supersede the Arduino's onboard ADC, may give more frequent and accurate sampling of transducer outputs. Such an improvement could potentially allow for more detailed analysis of amalgam separator functionality. Additionally, an improved user interface may reduce computing difficulties and unforeseen complications with data retrieval. The possibilities for additional applications that stem from this technology are numerous and will positively impact both the military and public sectors.

Appendix I: TERMINOLOGY AND WORKING DEFINITIONS

This section briefly explains computational science and engineering terminology necessary to understand the sensor's design and function.

- Inches of Hg refers to a pressure unit. At 32°F, the pressure induced on the bottom of a 1 inch Hg column is equivalent to 1 inch of Hg in pressure.
- SPI refers to Serial Peripheral Interface which is a non-standardized communication method between electronic devices. Generally, a device that uses SPI will have a pin dedicated to communicating with another device, a pin dedicated to listening to that device, a clock signal to keep pace for the data transfer, and a pin which turns on and off the communication.
- I²C refers to Inter-Integrated Circuit, a communication protocol licensed by NXP Semiconductors. The protocol allows for many devices to communicate across two lines by using an address system maintained by NXP Semiconductors.
- Transducers are devices that convert some physical phenomena to an electrical signal of a predefined range. The electrical signal used can be a current or a voltage in reference to a common ground. The range of data is usually continuous in the analog fashion.
- VDC refers to direct-current voltage.
- VAC refers to voltage with alternating current.
- GB refers to a gigabyte of data.
- SD refers to a memory card that uses solid-state storage.
- FAT16 and FAT32 refer to types of memory storage present on a SD card.
- I/O is an alias of the external inputs and outputs of an integrated circuit or computer.
- A data string is a series of characters that is manipulated by a computer program. These characters can represent words, sentences, numbers, and anything else which can be typed on a keyboard.

- BSPP refers to British Standard Pipe Parallel which is a type of threading used in pipe fittings. These fittings are defined in imperial units and correspond to the internal diameter of a female-end fitting.
- NPT refers to the National Pipe Thread Taper, which is another type of threading used in pipe fittings. These fittings are also defined in Imperial units and correspond to the internal diameter of the female-end fitting. The threading in the fittings is tapered, meaning that there is an angle in the threading converging away from the opening.
- Arduino IDE refers to the version 1.6.4 of the Arduino internal development environment. The IDE is used to create and load user created programs onto the Arduino microcontroller connected with an USB A to USB B cord. The Arduino IDE also provides a serial monitor to a connected Arduino microcontroller to transmit readable messages to and from a computer.
- Real-time clock (RTC) is an integrated circuit that keeps a running clock, which corresponds to the date and time one would find on a wall clock and calendar. RTCs are usually paired with a rechargeable battery to power the circuit when the main power supply is cut off.
- Analog-to-digital converter (ADC) refers to a component that converts an analog electrical signal to a digital signal representing a range of natural numbers. The length of this range is usually in a power of 2, such as 1024, minus any offset due to design limitations.

Appendix II: CIRCUIT DIAGRAM

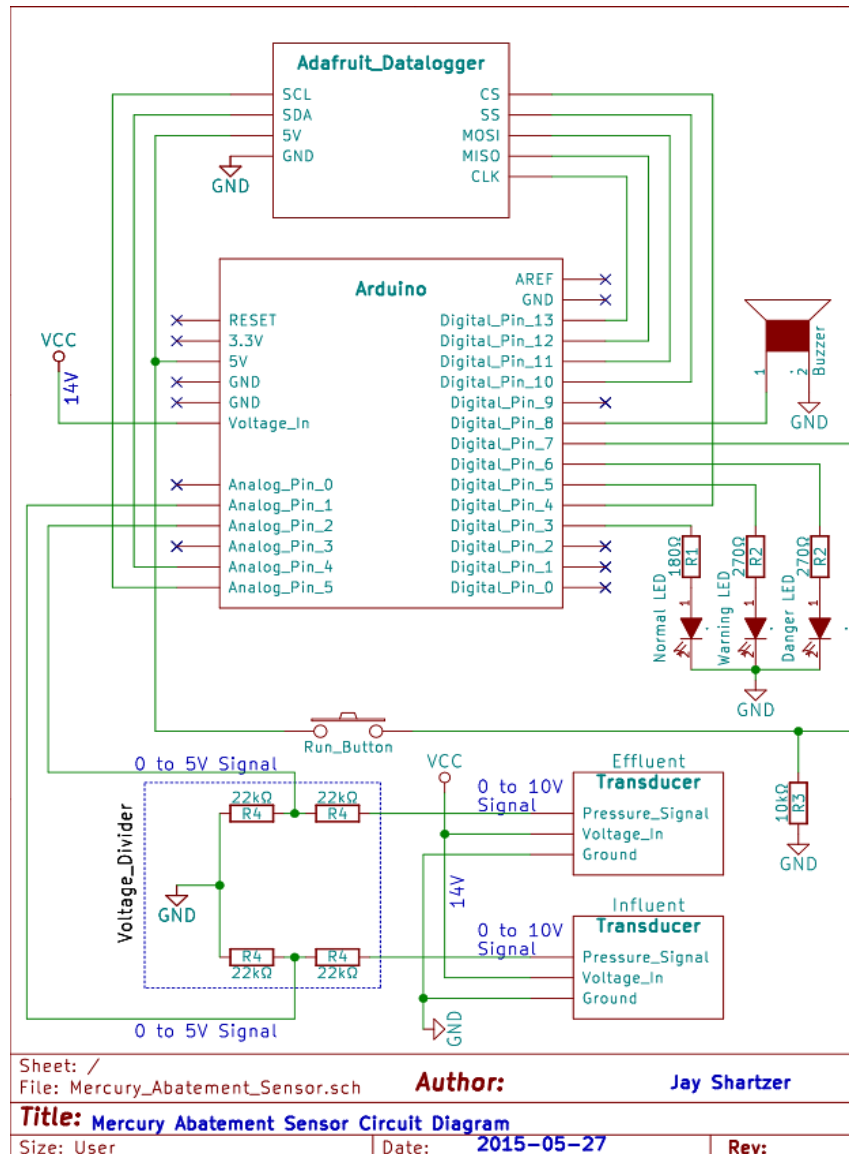


Figure 14: Sensor circuit diagram. This diagram is not to scale. Electrical pins with an “X” were not used. VCC: Voltage Common Connection. GND: common electrical ground. I²C communication: Serial Clock Line (SCL), Serial Data Line (SDA), Analog_Pins_4, and 5. SPI communication: Chip Select (CS), Slave Select (SS), Master Out Slave In (MOSI), Master In Slave Out (MISO), and Cloak (CLK). The inflow and outflow transducers are represented with the connections Pressure_Signal, Voltage_In, and Ground.

Appendix III: PROGRAM FLOW CHART

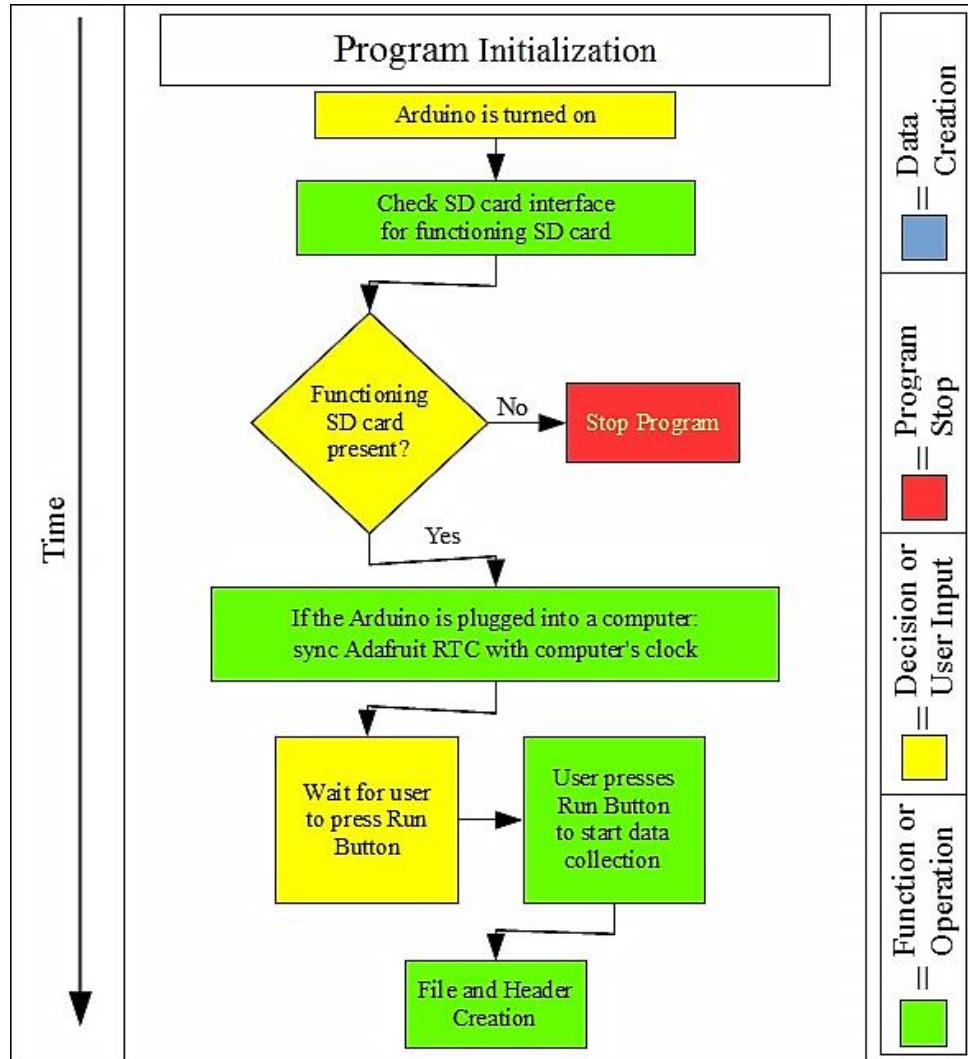


Figure 15. Initialization portion of the sensor program shown conceptually. This portion of the program will run once when the sensor is first powered and prepares the sensor to begin data collection. The color legend to the right categorizes each step of the algorithm according to function.

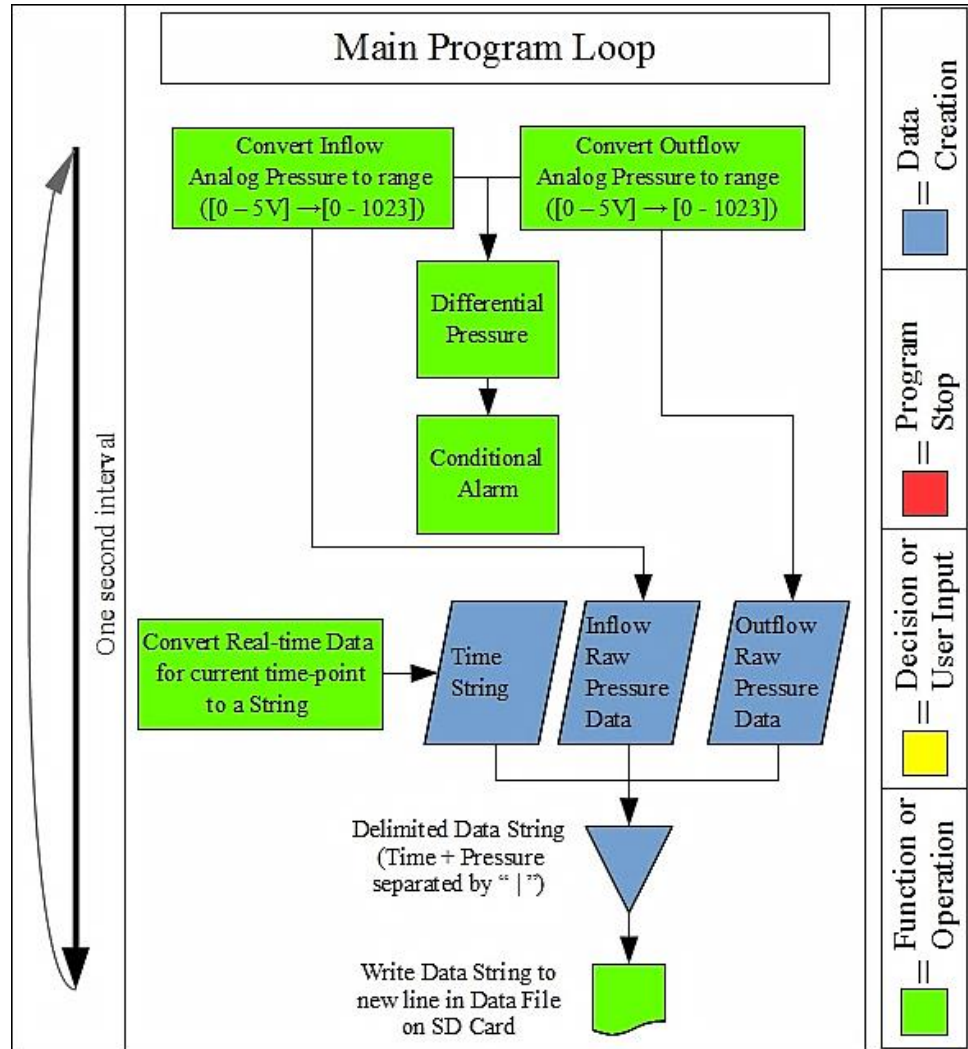


Figure 16. Functional diagram displaying the part of the program on the Arduino as it processes incoming data, activates any necessary alarms, and transfers the data to the attached SD card. This process continues looping until the reset button on the Arduino is pressed or the Arduino is shut down. The color legend to the right categorizes each step of the algorithm according to function.

Appendix IV: TRANSDUCER CONVERSION COMPARED TO RG-1

Reference Gauge Output (inches of Hg)	Analog-to-Digital Conversion of Pressure Transducer Output									
	Sampling Date									
	7/6/2015		7/8/2015		7/9/2015					
	Inflow	Outflow	Inflow	Outflow	Inflow	Outflow	Inflow	Outflow	Inflow	Outflow
-1.103	1021	1002	1020	1001	1020	1001	1020.33	1001.33	0.19	0.19
-1.471	1008	990	1007	989	1006	989	1007.00	989.33	0.58	0.19
-1.839	994	978	996	976	994	975	994.67	976.33	1.02	0.69
-2.207	983	965	983	964	981	964	982.33	964.33	1.02	0.19
-2.574	971	952	969	952	967	950	969.00	951.33	1.15	1.02
-2.942	958	939	956	938	955	937	956.33	938.00	0.69	0.58
-3.310	946	928	945	926	943	925	944.67	926.33	1.07	0.69
-3.678	935	915	933	913	931	913	933.00	913.67	1.15	0.38
-4.045	921	903	919	901	919	901	919.67	901.67	0.38	0.38
-4.413	908	890	907	888	905	887	906.67	888.33	1.07	0.69
-4.781	895	877	893	875	891	874	893.00	875.33	1.15	0.69
-5.149	883	864	881	862	879	861	881.00	862.33	1.15	0.69
-5.517	870	851	862	849	867	849	866.33	849.67	2.71	0.38
-5.884	857	838	856	837	852	835	855.00	836.67	2.08	1.07
-6.252	843	824	843	824	841	823	842.33	823.67	1.02	0.51
-6.620	831	811	830	811	828	809	829.67	810.33	1.07	1.02
-6.988	816	798	815	797	815	797	815.33	797.33	0.19	0.19

Table 1. RG-1 vs Ashcroft Transducer data retrieved during three sets of calibration testing.

REFERENCES

- [1] J. F. Risher, “Elemental Mercury and Inorganic Mercury Compounds: Human Health Aspects.” World Health Organization, 2003.
- [2] M. G. Rasines Alcaraz, A. Veitz-Keenan, P. Sahrman, P. R. Schmidlin, D. Davis, and Z. Iheozor-Ejiofor, “Direct composite resin fillings versus amalgam fillings for permanent or adult posterior teeth,” in *Cochrane Database of Systematic Reviews*, The Cochrane Collaboration, Ed. Chichester, UK: John Wiley & Sons, Ltd, 2014.
- [3] J. D. Overton and D. J. Sullivan, “Early Failure of Class II Resin Composite Versus Class II Amalgam Restorations Placed by Dental Students,” *J. Dent. Educ.*, vol. 76, no. 3, pp. 338–340, Mar. 2012.
- [4] U.S. Food and Drug Administration, “About Dental Amalgam Fillings,” *www.fda.gov*, 10-Feb-2015. [Online]. Available: <http://www.fda.gov/MedicalDevices/ProductsandMedicalProcedures/DentalProducts/DentalAmalgam/ucm171094.htm>. [Accessed: 24-Jul-2015].
- [5] J. L. Drummond, M. D. Cailas, and K. Croke, “Mercury Generation Potential from Dental Waste Amalgam,” *J. Dent.*, vol. 31, no. 7, pp. 493–501, Sep. 2003.
- [6] X. Zhao, K. J. Rockne, J. L. Drummond, R. K. Hurley, C. W. Shade, and R. J. Hudson, “Characterization of Methyl mercury in Dental Wastewater and Correlation with Sulfate-reducing Bacterial DNA,” *Env. Sci Technol*, vol. 42, no. 8, pp. 2780–6, Apr. 2008.
- [7] “Effluent Limitations Guidelines and Standards for the Dental Category.” Environmental Protection Agency, Sep-2014.
- [8] “Dental Effluent Guidelines,” *water.epa.gov*, 25-Feb-2015. [Online]. Available: <http://water.epa.gov/scitech/wastetech/guide/dental/index.cfm>. [Accessed: 15-Sep-2015].
- [9] “Mercury in Dental Amalgam,” *www.epa.gov*, 29-Dec-2014. [Online]. Available: <http://www.epa.gov/mercury/dentalamalgam.html>. [Accessed: 22-Jul-2015].
- [10] B. Muhamedagic, L. Muhamedagic, and I. Masic, “Dental Office Waste - Public Health and Ecological Risk,” *Mater Sociomed*, vol. 21, no. 1, pp. 35–8, 2009.
- [11] L. D. Hylander, A. Lindvall, and L. Gahnberg, “High Mercury Emissions from Dental Clinics Despite Amalgam Separators,” *Sci. Total Environ.*, vol. 362, no. 1–3, pp. 74–84, Jun. 2006.
- [12] J. L. Drummond, Y. Liu, T.-Y. Wu, and M. D. Cailas, “Particle Versus Mercury Removal Efficiency of Amalgam Separators,” *J. Dent.*, vol. 31, no. 1, pp. 51–58, Jan. 2003.
- [13] “The International System of Units (SI) – Conversion Factors for General Use,” National Institute of Standards and Technology, NIST Special Publication 1038, May 2006.
- [14] “Ashcroft Instruments GmbH | PRODUKTE,” *www.ashcroft.eu*. [Online]. Available: <http://www.ashcroft.eu/english/products/produkte-include.html?pid=58>. [Accessed: 13-May-2015].
- [15] Swagelok, “Industrial Pressure Transducers.” Swagelok Company, Apr-2011.
- [16] “Getting Started with Arduino,” *www.arduino.cc*, 2015. [Online]. Available: <https://www.arduino.cc/en/Guide/HomePage>. [Accessed: 22-Jul-2015].
- [17] “UM10204 I2C-bus Specification and User Manual.” NXP Semiconductors, 04-Apr-2014.

- [18] J. W. Nilsson and S. A. Riedel, *Electric Circuits*, 9th ed. Boston: Prentice Hall, 2011.
- [19] “Date and Time Format - ISO 8601,” *www.iso.org*, 01-Dec-2004. [Online]. Available: <http://www.iso.org/iso/home/standards/iso8601.htm>. [Accessed: 21-Jul-2015].